SAND2017-11553C

A Method for Canceling Force Transducer Mass and Inertia Effects

Lopp, Garrett K. * Pacini, Benjamin R.
Mayes, Randall L. †

October 16, 2017

Abstract

Experimental modal analysis via shaker testing introduces errors in the measured structural response that can be attributed to the force transducer assembly fixed on the vibrating structure. Previous studies developed transducer mass-cancellation techniques for systems with translational degrees of freedom; however, studies addressing this problem when rotations cannot be neglected are sparse. In situations where rotations cannot be neglected, the apparent mass of the transducer is dependent on its geometry and is not the same in all directions. This paper investigates a method for correcting the measured system response that is contaminated with the effects the attached force transducer mass and inertia. Experimental modal substructuring facilitated estimations of the translational and rotational mode shapes at the transducer connection point, thus enabling removal of an analytical transducer model from the measured test structures resulting in the corrected response. A numerical analysis showed the feasibility of the proposed approach in estimating the correct modal frequencies and forced response. To provide further validation, an experimental analysis showed the proposed approach applied to results obtained from a shaker test more accurately reflected results obtained from a hammer test.

1 INTRODUCTION

Conducting a modal test with a vibration shaker offers many benefits over impact testing; however, one drawback includes the requirement of a force transducer fixed on the vibrating structure. If the structure is relatively lightweight, the presence of this transducer can alter the structure's mass distribution, thus affecting the dynamic response and driving down the modal frequency estimates. The mass-cancellation procedure for transducers at drive-point measurements has been well-known for some time [1]. More recently, methods have been developed to extend the correction for transfer measurements. [2, 3, 4, 5, 6, 7, 8] Although showing success, these methods mainly focus on eliminating the transducer mass effects from the dynamic response. For systems where rotations cannot be neglected, such as beam- and plate-like structures, 75% of the frequency response function (FRF) matrix corresponds to rotation-based quantities, so the transducer inertia can also pollute the dynamic response. [9] The focus of the current paper is to develop a suitable approach capable of correcting for the both the transducer mass and inertia on the measured response.

The proposed approach utilizes concepts from an experimental modal substructuring approach introduced by Allen et al [10, 11] that utilizes a fixture attached to a test article for the purpose of combining with an analytical model of a separate substructure. Inclusion of this fixture mass-loads the test article interface which leads to an improved modal basis and more accurate modal parameter estimates when combining with the analytical substructure. The fixture is of simple geometry so that an accurate analytical model facilitates the removal of the fixture effects from the final combined system. The current paper adopts this concept by incorporating an analytical model of a local section of the test structure containing the attached force transducer. Rather than using the local analytical model to remove the effects of the substructure from the system response, the model is instead used in an expansion process to estimate the mode shapes corresponding to both translation and rotation degrees of freedom at the transducer connection point. An accurate estimation of these connection

*Graduate Research Assistant, Department of Mechanical and Aerospace Engineering, University of Central Florida, Orlando, FL, 32816
†Structural Dynamics Department, Sandia National Laboratories, Albuquerque, NM, 87185

point mode shapes, combined with a rigid body model of the force transducer, enables immediately removal of the force transducer from the system.

The remainder of the paper is composed as follows: Section 2 develops the substructuring theory used to remove the transducer effects. Also provided is a discussion on modeling the force transducer as a general rigid body. Section 3 introduces the test structure utilized in this work. Simulations are then performed on a 2-D finite element (FE) model with an attached force transducer to test the performance of correction approach. The results are then compared to a similar model without the transducer in terms of the modal frequencies, as well as the forced response. Section 4 provides experimental validation of the proposed approach by correcting the response obtained from a shaker test. The results are then compared to a hammer test on the same structure without the force transducer assembly.

2 THEORETICAL DEVELOPMENT

2.1 Transducer Removal

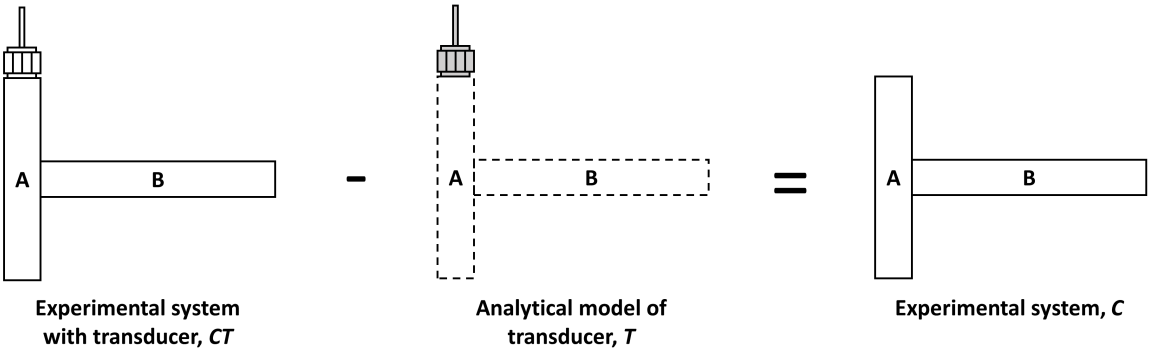

Figure 1: Example of transducer removal from experimental system.

Consider the T-Beam structure shown in Fig. 1. When performing a shaker vibration test, the effects of the mass and inertia of the attached force transducer on the test structure, specified here as CT, pollute the measured data. The approach presented here assumes the force transducer, specified here as component T, is a rigid body with a mass and inertia that can be determined leading to an analytical mass matrix. Subtracting the mass matrix of the force transducer from the measured system recovers the true system without the transducer, specified here as system C. The equations of motion governing this process are

$$\begin{bmatrix} \mathbf{M}_{CT} & \mathbf{0} \\ \mathbf{0} & -\mathbf{M}_T \end{bmatrix} \begin{Bmatrix} \ddot{\mathbf{u}}_{CT} \\ \ddot{\mathbf{u}}_T \end{Bmatrix} + \begin{bmatrix} \mathbf{C}_{CT} & \mathbf{0} \\ \mathbf{0} & \mathbf{0} \end{bmatrix} \begin{Bmatrix} \dot{\mathbf{u}}_{CT} \\ \dot{\mathbf{u}}_T \end{Bmatrix} + \begin{bmatrix} \mathbf{K}_{CT} & \mathbf{0} \\ \mathbf{0} & \mathbf{0} \end{bmatrix} \begin{Bmatrix} \mathbf{u}_{CT} \\ \mathbf{u}_T \end{Bmatrix} = \begin{Bmatrix} \mathbf{f}_{CT} \\ \mathbf{0} \end{Bmatrix} + \begin{Bmatrix} \mathbf{g}_{CT} \\ \mathbf{g}_T \end{Bmatrix} \tag{1}$$

where $\mathbf{u}$ is the 3-D response vector containing both translations and rotations at each element node, and the subscripts CT and T refer to quantities associated with the test structure CT and transducer T, respectively. The above equations are also subject to constraints at the transducer connection point where the motion between the transducer and the system are equal and the reaction forces are equal and opposite. These constraints are

$$\mathbf{B} \begin{Bmatrix} \mathbf{u}_{CT} \\ \mathbf{u}_T \end{Bmatrix} = 0 \tag{2}$$

$$\mathbf{L}^T \begin{Bmatrix} \mathbf{g}_{CT} \\ \mathbf{g}_T \end{Bmatrix} = 0 \tag{3}$$

The force transducer can be idealized with a simple geometry allowing for an analytical calculation of the mass matrix M_T; however, the spatial model for CT is unknown. Instead, a modal model for CT is derived from a modal test. Transforming the equations of motion into the modal coordinate system

using the R_{CT} frequencies and mass-normalized mode shapes for the system ($\omega_{CT,r}$ and $\phi_{CT,r}$), as well as the R_T mass-normalized transducer rigid body modes ($\omega_{T,r} = 0$ and ϕ_T). The transformation to the modal coordinate system is

$$\begin{Bmatrix} \mathbf{u}_{CT} \\ \mathbf{u}_T \end{Bmatrix} = \begin{bmatrix} \mathbf{\Phi}_{CT} & \mathbf{0} \\ \mathbf{0} & \mathbf{\Phi}_T \end{bmatrix} \begin{Bmatrix} \mathbf{q}_{CT} \\ \mathbf{q}_T \end{Bmatrix} \tag{4}$$

with the associated modal equations of motion

$$\begin{aligned} \begin{bmatrix} \mathbf{I}_{CT} & \mathbf{0} \\ \mathbf{0} & -\mathbf{I}_T \end{bmatrix} \begin{Bmatrix} \ddot{\mathbf{q}}_{CT} \\ \ddot{\mathbf{q}}_T \end{Bmatrix} + \begin{bmatrix} [\backslash 2\zeta_r\omega_r\backslash]_{CT} & \mathbf{0} \\ \mathbf{0} & \mathbf{0} \end{bmatrix} \begin{Bmatrix} \dot{\mathbf{q}}_{CT} \\ \dot{\mathbf{q}}_T \end{Bmatrix} + \begin{bmatrix} [\backslash \omega_r^2 \backslash]_{CT} & \mathbf{0} \\ \mathbf{0} & \mathbf{0} \end{bmatrix} \begin{Bmatrix} \mathbf{q}_{CT} \\ \mathbf{q}_T \end{Bmatrix} \\ = \begin{Bmatrix} {\mathbf{\Phi}_{CT}}^T \mathbf{f}_{CT} \\ \mathbf{0} \end{Bmatrix} + \begin{bmatrix} {\mathbf{\Phi}_{CT}}^T & \mathbf{0} \\ \mathbf{0} & {\mathbf{\Phi}_T}^T \end{bmatrix} \begin{Bmatrix} \mathbf{g}_{CT} \\ \mathbf{g}_T \end{Bmatrix} \end{aligned} \tag{5}$$

The corresponding modal constraint equations are then

$$\mathbf{B} \begin{bmatrix} \mathbf{\Phi}_{CT} & \mathbf{0} \\ \mathbf{0} & \mathbf{\Phi}_T \end{bmatrix} \begin{Bmatrix} \mathbf{q}_{CT} \\ \mathbf{q}_T \end{Bmatrix} = 0 \tag{6}$$

$${\mathbf{L}_p}^T \begin{bmatrix} {\mathbf{\Phi}_{CT}}^T & \mathbf{0} \\ \mathbf{0} & {\mathbf{\Phi}_T}^T \end{bmatrix} \begin{Bmatrix} \mathbf{g}_{CT} \\ \mathbf{g}_T \end{Bmatrix} = 0 \tag{7}$$

Enforcing the modal compatibility constraint of Eq. 6 requires knowledge of the mode shapes of system CT, including rotational degrees of freedom, at the transducer connection point (i.e., $\mathbf{\Phi}_{CT,T}$ must be fully known); such knowledge may not be available in a typical modal test. Instead, enforcing these modal constraints between the experimental system and the analytical transducer model requires a separate approach. The approach proposed here assumes that a simple analytical model AT can adequately describe the motion of a local section of the experimental system containing the force transducer attachment (e.g., the vertical beam in Fig. 1). By measuring translations on this local system, the analytical model then generates information regarding motion at the transducer connection point. This process begins by first constraining the measurement points, denoted with the m subscript, between AT and CT such that

$$\mathbf{u}_{AT,m} = \mathbf{u}_{CT,m} \tag{8}$$

or in the modal coordinate system

$$\mathbf{\Phi}_{AT,m}\mathbf{q}_{AT} = \mathbf{\Phi}_{CT,m}\mathbf{q}_{CT} \tag{9}$$

Taking the pseudo-inverse (denoted with the † superscript) of the analytical mode shape matrix at the measurement points produces a least-squares fit for the modal motion of AT in terms of the modal response of CT

$$\mathbf{q}_{AT} = {\mathbf{\Phi}_{AT,m}}^\dagger \mathbf{\Phi}_{CT,m}\mathbf{q}_{CT} \tag{10}$$

The application of the pseudo-inverse requires at least as many measurements on AT as there are modes included in the model (i.e., $m > R_{AT}$). This process is the basis of the modal constraints for fixture and subsystem *MCFS* substructure constraint approach. [10, 11]. However, rather than using these modal constraints to remove AT from system CT, the analytical mode shapes of AT allow for an expansion of the modal response to estimate the motion at the transducer connection point

$$\mathbf{u}_{AT,T} = \mathbf{\Phi}_{AT,T}\mathbf{q}_{AT} \tag{11}$$

Substituting $\mathbf{q}_{AT}$ from Eq. 10 into the above equation leads to

$$\mathbf{u}_{AT,T} = \underbrace{\left[\mathbf{\Phi}_{AT,T}{\mathbf{\Phi}_{AT,m}}^\dagger \mathbf{\Phi}_{CT,m}\right]}_{\hat{\mathbf{\Phi}}_{CT,T}} \mathbf{q}_{CT} = \hat{\mathbf{u}}_{CT,T} \tag{12}$$

The bracketed terms are the estimated system CT mode shapes that correspond to the transducer connection point degrees of freedom $\hat{\mathbf{\Phi}}_{CT,T}$ and are generated using a combination of the system CT measured mode shapes and analytical system AT mode shapes. Essentially, this process can then be thought of as first applying a modal filter to obtain the modal response of system AT from

the translation measurements on system CT, followed by a model expansion to obtain the motion (translations and rotations) at the transducer connection point. This process allows for the motion of the force transducer to be constrained to system AT at the transducer connection point

$$\mathbf{u}_{AT,T} = \mathbf{u}_T \tag{13}$$

or rewritten in terms of the modal response of T

$$\mathbf{u}_{AT,T} = \mathbf{\Phi}_T \mathbf{q}_T \tag{14}$$

Inserting the above equation into Eq. 12 and rearranging leads to an equation constraining the transducer modal response with that of the measured system

$$\hat{\mathbf{\Phi}}_{CT,T}\mathbf{q}_{CT} - \mathbf{\Phi}_T\mathbf{q}_T = \mathbf{0} \tag{15}$$

The constraints can be written in terms of the modal constraint matrix $\mathbf{B}_p$ such that

$$\underbrace{\begin{bmatrix}\hat{\mathbf{\Phi}}_{CT,T} & -\mathbf{\Phi}_T\end{bmatrix}}_{\mathbf{B}_p}\begin{Bmatrix}\mathbf{q}_{\mathrm{CT}}\\ \mathbf{q}_T\end{Bmatrix} = \mathbf{0} \tag{16}$$

where $\mathbf{B}_p$ enforces as many constraints as the number of degrees of freedom N_T in the transducer model; for the general case of 3-D motion, this corresponds to three translations and three rotations, so $N_T = 6$. From Eq. 5, there are $R_{CT} + R_T$ equations and, using all the rigid body modes of the transducer, there are R_T constraints, thus requiring a transformation to an unconstrained set of modes. Choosing this set simply as the modes of CT, the transformation is

$$\begin{Bmatrix}\mathbf{q}_{CT}\\ \mathbf{q}_T\end{Bmatrix} = \underbrace{\begin{bmatrix}\mathbf{I}_{CT}\\ {\mathbf{\Phi}_T}^{-1}\hat{\mathbf{\Phi}}_{CT,T}\end{bmatrix}}_{\mathbf{L}_p}\mathbf{q}_{CT} \tag{17}$$

where $\mathbf{L}_p$ is the transformation matrix that is in the null space of $\mathbf{B}_p$, thus always satisfying the constraints of Eq. 16. Inserting this transformation into Eq. 5 and premultiplying by $\mathbf{L}_p^T$ results in the unconstrained equations

$$\tilde{\mathbf{M}}\ddot{\mathbf{q}}_{CT} + \tilde{\mathbf{C}}\dot{\mathbf{q}}_{CT} + \tilde{\mathbf{K}}\mathbf{q}_{CT} = \tilde{\mathbf{f}} + \tilde{\mathbf{g}} \tag{18}$$

where

$$\tilde{\mathbf{M}} = {\mathbf{L}_p}^T\begin{bmatrix}\mathbf{I}_{\mathrm{C}} & \mathbf{0}\\ \mathbf{0} & -\mathbf{I}_T\end{bmatrix}\mathbf{L}_p = \mathbf{I}_{CT} - \hat{\mathbf{\Phi}}_{CT,T}^T\left[\mathbf{\Phi}_T{\mathbf{\Phi}_T}^T\right]^{-1}\hat{\mathbf{\Phi}}_{CT,T} \tag{19}$$

$$\tilde{\mathbf{C}} = {\mathbf{L}_p}^T\begin{bmatrix}[\backslash 2\zeta_r\omega_r\backslash]_{CT} & \mathbf{0}\\ \mathbf{0} & \mathbf{0}\end{bmatrix}\mathbf{L}_p = [\backslash 2\zeta_r\omega_r\backslash]_{CT} \tag{20}$$

$$\tilde{\mathbf{K}} = {\mathbf{L}_p}^T\begin{bmatrix}[\backslash \omega_r^2\backslash]_{CT} & \mathbf{0}\\ \mathbf{0} & \mathbf{0}\end{bmatrix}\mathbf{L}_p = [\backslash \omega_r^2\backslash]_{CT} \tag{21}$$

$$\tilde{\mathbf{f}} = {\mathbf{L}_p}^T\begin{Bmatrix}{\mathbf{\Phi}_{CT}}^T\mathbf{f}_{CT}\\ \mathbf{0}\end{Bmatrix} = {\mathbf{\Phi}_{CT}}^T\mathbf{f}_{CT} \tag{22}$$

$$\tilde{\mathbf{g}} = {\mathbf{L}_p}^T\begin{bmatrix}{\mathbf{\Phi}_{CT}}^T & \mathbf{0}\\ \mathbf{0} & {\mathbf{\Phi}_T}^T\end{bmatrix}\begin{Bmatrix}\mathbf{g}_{CT}\\ \mathbf{g}_T\end{Bmatrix} = \mathbf{0} \tag{23}$$

The updated modal damping matrix $\tilde{C}$, stiffness matrix $\tilde{K}$, and modal force vector $\tilde{f}$ remain unchanged from the initial measured system; however, the modal mass matrix $\tilde{M}$ is reduced by an amount that corresponds to the removal of the force transducer. Expanding this mass matrix further results in

$$\tilde{\mathbf{M}} = \mathbf{I}_{CT} - \mathbf{\Phi}_{CT,m}^T\left[\left(\mathbf{\Phi}_{AT,T}{\mathbf{\Phi}_{AT,m}}^\dagger\right)^T\left(\mathbf{\Phi}_T{\mathbf{\Phi}_T}^T\right)^{-1}\mathbf{\Phi}_{AT,T}{\mathbf{\Phi}_{AT,m}}^\dagger\right]\mathbf{\Phi}_{CT,m} \tag{24}$$

The bracketed term in the above equation is pre- and post-multiplied by $\mathbf{\Phi}_{CT,m}^T$ and $\mathbf{\Phi}_{CT,m}$, indicating mass is removed from the measurement locations on CT. Essentially, the above process utilizes the analytical modes of AT and T to eliminate the requirement for directly measuring mode shapes corresponding to the rotation degrees of freedom at the transducer connection point. The force transducer mass and inertia are then distributed as an equivalent mass at the translation measurement locations, thus allowing for immediate removal from the system.

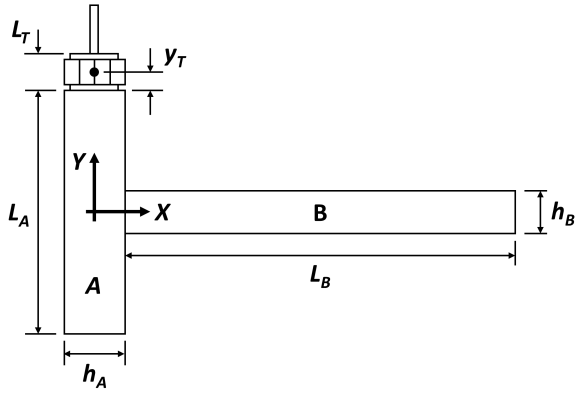

Figure 2: System of interest with attached transducer.

2.2 Transducer Model

The current approach utilizes the mass-normalized rigid body modes of the force transducer and requires a model that accurately describes the rigid body dynamics. This analysis assumes the transducer behaves as a general rigid body connected to a single point on the surface of the structure with the transducer center of mass offset a distance $r_T = (x_T, y_T, z_T)$. The mass matrix of a general rigid body with respect to the connection point on the surface of the structure is

$$\mathbf{M}_T = \begin{bmatrix} m_T & 0 & 0 & 0 & m_T z_T & -m_T y_T \\ 0 & m_T & 0 & -m_T z_T & 0 & m_T x_T \\ 0 & 0 & m_T & m_T y_T & -m_T x_T & 0 \\ 0 & -m_T z_T & m_T y_T & I_{xx} & -I_{xy} & -I_{xz} \\ m_T z_T & 0 & -m_T x_T & -I_{xy} & I_{yy} & -I_{yz} \\ -m_T y_T & m_T x_T & 0 & -I_{xz} & -I_{yz} & I_{zz} \end{bmatrix} \tag{25}$$

where m_T is the mass of the force transducer, I_{xx}, I_{yy}, and I_{zz} are the moments of inertia, and I_{xy}, I_{yz}, I_{xz} are the products of inertia about the coordinate system located at the connection point on the structure surface. Also note that only half of the transducer mass contributes to the force measurement as the terminal is located approximately halfway along the transducer thickness. In the above mass matrix, only half of the transducer mass needs to be included in the direction in-line with the applied force; for the perpendicular directions, the total mass of the transducer should be used. Furthermore, the geometry of the transducer used in the proceeding sections is idealized as a solid uniform cylinder allowing analytical calculations of the inertia terms. The transducer mass-normalized rigid body modes can then be determined.

3 Numerical Simulations

3.1 System of Interest

To test the proposed approach, the T-beam system shown in Fig. 2 was utilized with the corresponding parameters recorded in Table 1. This analysis assumes the out-of-plane motion is negligible, thus reducing the system to 2-D that results in the transducer mass matrix

$$\mathbf{M}_T = \begin{bmatrix} m_T & 0 & -m_T y_T \\ 0 & m_T/2 & 0 \\ -m_T y_T & 0 & I_{zz} \end{bmatrix} \tag{26}$$

Note here the inclusion of only half of the transducer mass in the direction of the applied force reasons previously discussed.

3.2 Results

The numerical analysis utilized the finite element (FE) approach to model the system with 2-D beam elements where beams A and B contained 20 and 40 elements, respectively. Obtaining an adequate

Table 1: T-Beam System Parameters

Beam A		**Beam** B		**Force Transducer** T	
Material	Steel	Material	Steel	Mass	0.05 lbs
$L_A \times w_A \times h_A$	$4.5 \times 1 \times 1$ in^3	$L_B \times w_B \times h_B$	$12 \times 1 \times 0.75$ in^3	Inertia about C.M.	0.0036 lbs in^2

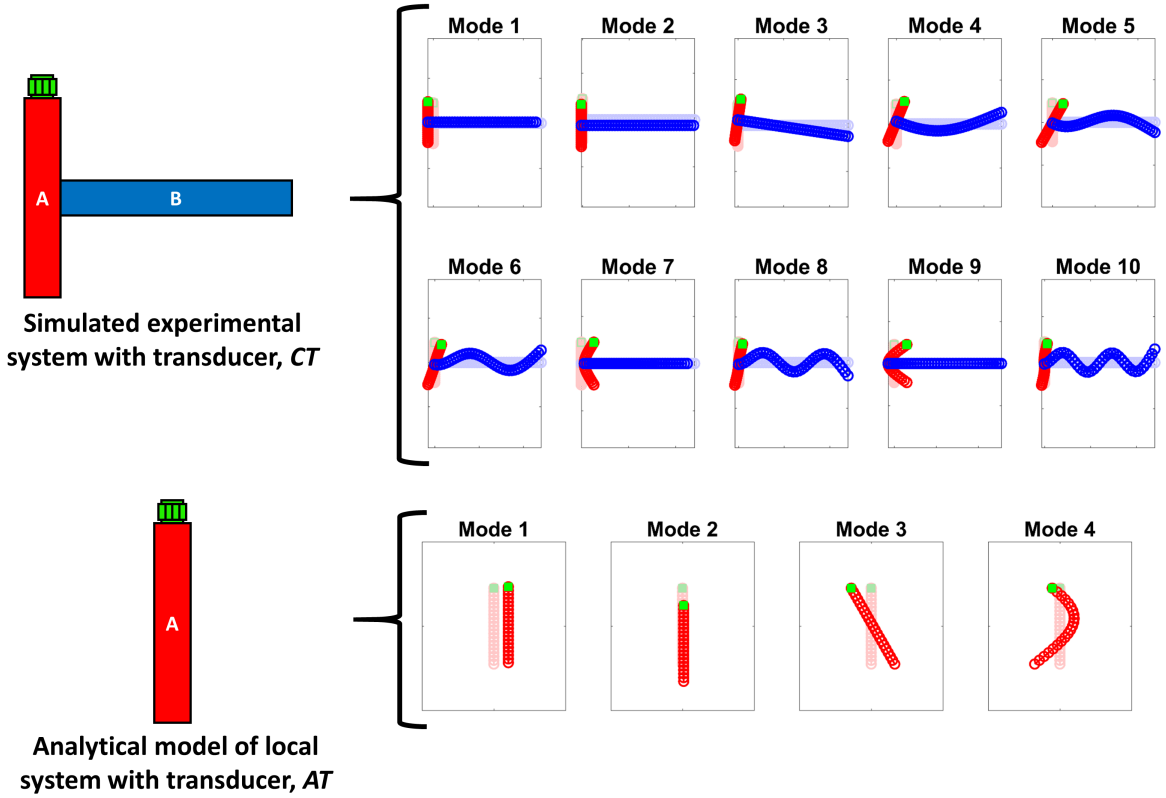

Figure 3: Mode shapes generated from the FE model for the (top) simulated experimental system with the attached transducer and the (bottom) analytical model of the local portion of the system that contains the transducer.

estimate of the mode shapes at the transducer connection point ($\hat{\mathbf{\Phi}}_{CT,T}$ in Eq. 12) requires a sufficient number of modes of the analytical beam AT to capture the modal motion of the local section of system CT that contains the transducer. Figure 3 shows the first 10 mode shapes (3 rigid body modes and 7 elastic modes) of CT. The vertical beam A shows mostly rigid body motion for each mode, as well as first beam bending motion for modes 7 and 9. Figure 3 shows the first four modes shapes (3 rigid body modes and one elastic mode) of AT required to form a sufficient modal basis for the local modal motion on CT.

To simulate an experimental test, translation measurements in both in-plane directions were recorded at 3 locations along AT, two at the beam tips and one at the beam center. Figure 4 shows an example of the process used to estimate the mode shapes at the transducer connection point for mode 7 of CT. Also shown is the estimated mode shape of the vertical section generated by the mode shapes at the measurement locations on CT, and the analytical mode shapes of AT given by

$$\hat{\mathbf{\Phi}}_{CT} = \mathbf{\Phi}_{AT}\mathbf{\Phi}_{AT,m}{}^{\dagger}\mathbf{\Phi}_{CT,m} \tag{27}$$

This estimated mode shape includes both translation and rotation information at every point along the vertical beam, including the transducer connection point, thus allowing for the removal of the transducer mass and inertia from each mode included in the system.

The transducer was then removed from the simulated experimental system CT using the process described in the previous section. The simulated experiment assumed all the modes of CT under 10 kHz are "measured" exactly with the first 10 modes falling within this frequency band. The first 4 modes of AT were then used in the transducer removal procedure. A FE model of the system

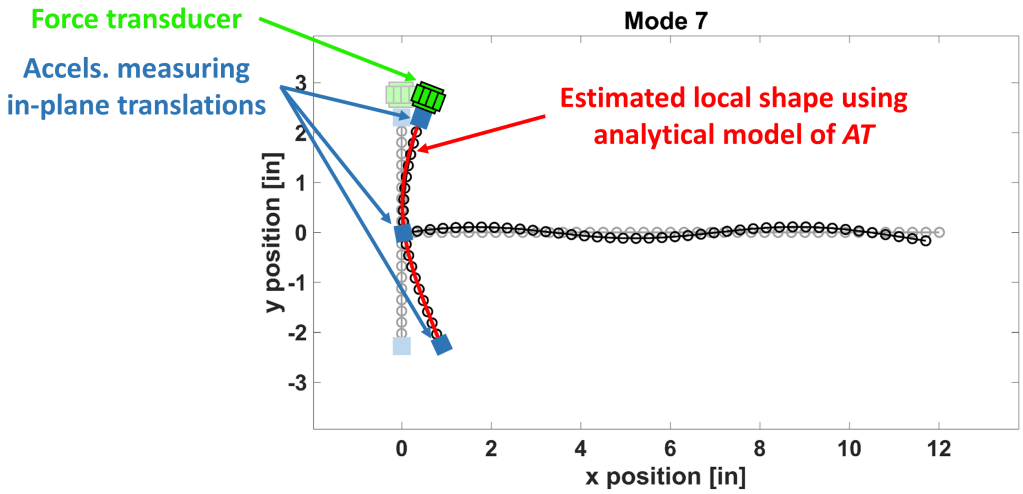

Figure 4: Example of the estimated mode shape (red) for mode 7 of CT. This shape was obtained using x-, y-translation measurements at three locations (blue squares) on the local section of the CT containing the force transducer.

without the transducer was used as the truth baseline and the corresponding modal frequencies are compared to the system with the attached transducer, both before and after the correction procedure, and recorded in Table 2. As expected, the presence of the force transducer drives down the modal frequencies with a maximum error of 5.36% for the 9th mode. After correcting for the transducer, the frequencies more accurately reflect the truth case with the maximum error reduced to just 0.56%.

Table 2: Modal frequency comparison between the baseline case without the attached transducer and the cases with the attached transducer, both uncorrected and correct.

Flexible Mode #	**f_n actual: FEM [Hz]**	**f_n with transducer: uncorrected [Hz]**	**% Error**	**f_n with transducer: corrected [Hz]**	**% Error**
1	723.17	708.42	-2.04	723.15	0.00
2	1723.7	1663.8	-3.48	1723.3	-0.03
3	3334.8	3290.1	-1.34	3333.6	-0.04
4	5340.7	5143.4	-3.69	5351.9	0.21
5	6033.2	6011.3	-0.36	6031.0	-0.04
6	9311.5	8812.5	-5.36	9363.3	0.56
7	9735.8	9723.5	-0.13	9731.4	-0.05

Analysis of the forced response also shows the effectiveness of the proposed approach. Figure 5a shows the drive-point FRF for each of the three cases with modal damping $\zeta = 0.1\%$ assigned for all modes. For the uncorrected system, the first three resonances and anti-resonances show clear shifts to lower frequencies. For the corrected case, the resonance peaks show excellent agreement to the truth case for all modes, although the anti-resonance locations begin to deviate after 7 kHz. As a general rule of thumb for modal substructuring, modal information should be included for 1.5 to 2 times the frequency band of interest for the final assembly [10]. As modal information up to 10 kHz was included in this analysis, one would expect accurate results up to 5-6.7 kHz, which is indeed the case. Figure 5b shows the complex modal indicator function (CMIF) for this single forcing configuration. Again, the uncorrected system shows clear downward shifts for the resonance frequencies. Interestingly, two spurious peaks are also present and correspond to the axial modes of the system. The presence of these peaks indicates the presence of the transducer breaks the symmetry of the structure, leading to an appreciable effect on the axial modes shapes that allows a transverse load to excite these modes. The corrected system again shows excellent agreement for all modes in the frequency band. The two spurious peaks were reduced in magnitude, though not fully eliminated. Although not shown here, increasing both the number of modes in the analytical model AT and measurement points showed further reductions for these spurious peaks.

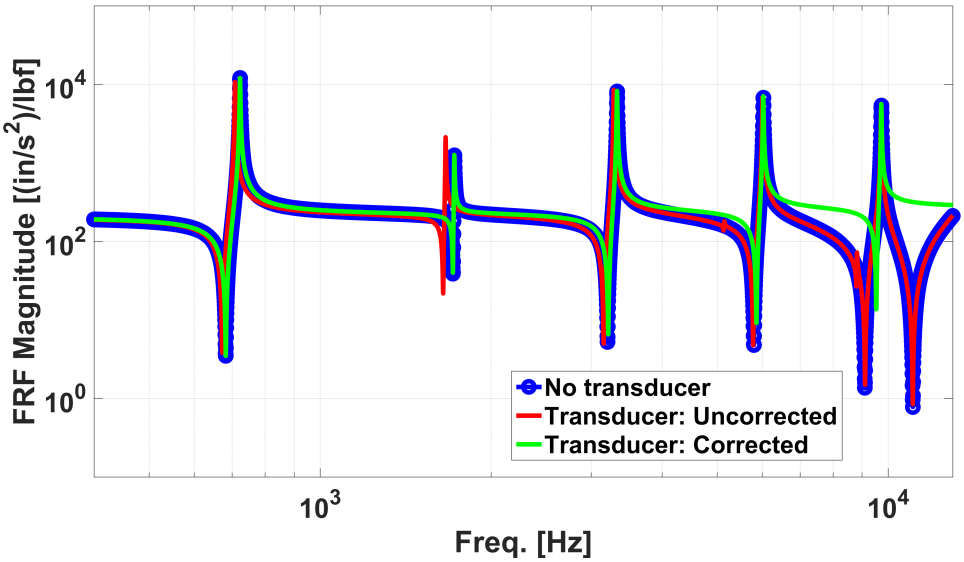

(a) Drive-point FRF.

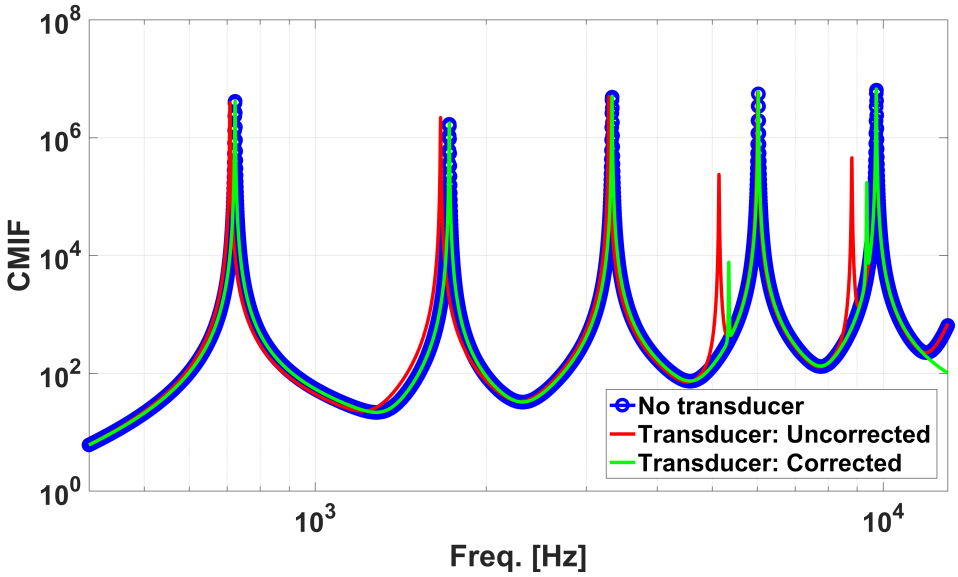

(b) Complex modal indicator function.

Figure 5: Frequency response for the truth baseline with no transducer (blue circles) and the system with the transducer, both uncorrected (red) and corrected using the proposed approach (green).

4 Experimental Results

Two separate modal tests were then performed to provide further validation for the proposed approach. Figure 6a shows the first test configuration, a hammer test that serves as the truth baseline without the attached transducer assembly. Figure 6b shows the second test configuration, a shaker test with the attached force transducer assembly. Excitation was provided up to 2.5 kHz to excite the first two in-plane bending modes. The response was measured with 9 triaxial accelerometers mounted on the structure, including 5 on the horizontal beam with the attached transducer.

The force transducer assembly consisted of not only the force transducer, but also a stinger adapter that has mass and inertia, idealized here as a solid cylinder, requiring removal from the system. A drive-cap was placed over an accelerometer used for drive-point measurements that introduces an offset of the transducer assembly from the test structure. This offset increases the inertia of the transducer assembly about the connection point and is accounted accounted for during the correction

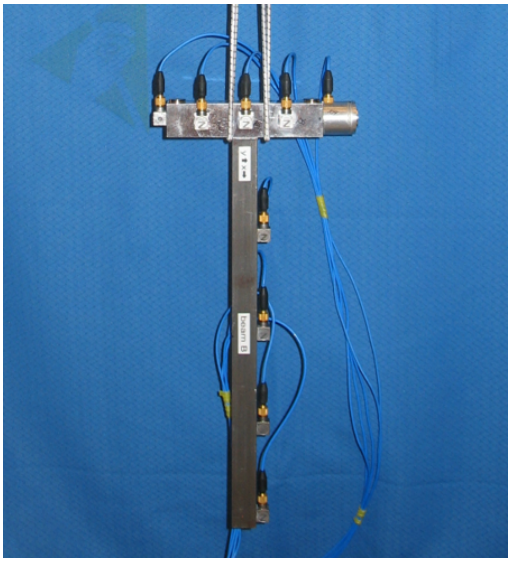

(a) Hammer test setup used as the truth baseline without the attached force transducer assembly.

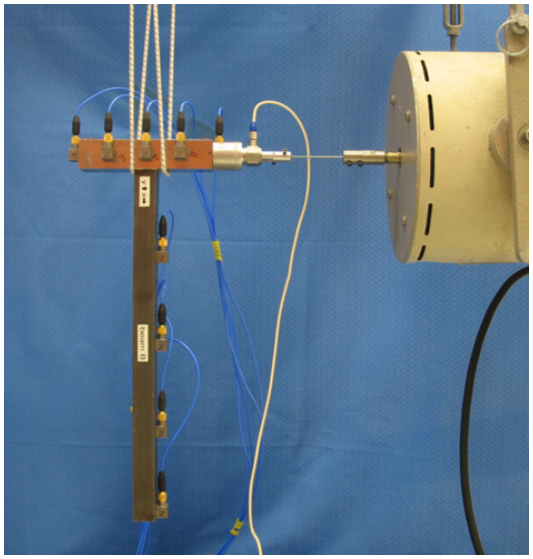

(b) Shaker test setup used to apply the transducer correction procedure.

Figure 6: Modal test configurations used to provide experimental validation.

procedure. Similar to the numerical simulations, the first 4 modes of the FE model shown in Fig. 3 were used for the horizontal beam to estimate the connection point mode shapes. Furthermore, the correction procedure utilized only 3 of the accelerometers located on the horizontal beam, the two located at the beam tips and the one located at the center of the beam closest to the vertical beam connection.

Table 3 shows a comparison of the modal frequencies. For the uncorrected shaker test, the first two modal frequencies showed downward shifts with errors of -4.44% and -7.81% for modes 1 and 2, respectively. After application of the correction procedure, the modal frequencies shifted upwards towards their true values with reduced errors of 1.41% and -0.48%.

The forced response was also analyzed for each of the cases. Figure 7a shows the drive-point FRFs where the uncorrected shaker response clearly shows the downward shifts for both the resonance and anti-resonance frequencies, as well as deviations in the peak response magnitudes. The corrected response shows drastic improvements for both the resonance and anti-resonance frequencies, as well as the peak magnitudes, though some deviations still exist. Figure 7b shows the CMIF where both the measured and synthesized singular values are shown for the hammer and uncorrected shaker tests. An out-of-plane bending mode can also be seen near 960 Hz, though was not synthesized in the modal parameter extraction process. The CMIF for the corrected shaker test shows excellent agreement with the hammer test, though again with some deviations in resonance frequency and the corresponding magnitude of the singular values. These deviations can most likely be attributed to the modeling of the force transducer assembly where both the force transducer, and the stinger adapter, were idealized as uniform cylinders; the associated cables and connector can also introduce mass and inertia that may not be negligible. Furthermore, it may be difficult to model completely the force transducer assembly and the response from a hammer test may not be available to compare the corrected shaker response. For such a case, one approach may be to develop a system with a simple geometry, such as the T-beam system used in this work, for the purpose of tuning the mass matrix for the force transducer assembly so that the corrected response from a shaker test matches more accurately the hammer test response. Such a calibration procedure will then garner more confidence when applying the correction for the same transducer assembly used on more complicated test structures.

5 Conclusions and Future Work

The objective of this paper was to correct for the force transducer mass and inertia effects during shaker tests. Utilizing concepts in experimental modal substructuring, this method relies on constraining the translation measurements on a local section of the test structure containing the transducer to

Table 3: Modal frequency comparison between the baseline case without the attached transducer and the cases with the attached transducer, both uncorrected and corrected.

Mode #	**Hammer: f_n truth [Hz]**	**Shaker: f_n uncorrected [Hz]**	**% Error**	**Shaker: f_n corrected [Hz]**	**% Error**
1	625.8	598.0	-4.44	634.6	1.41
2	1449	1344	-7.81	1442	-0.48

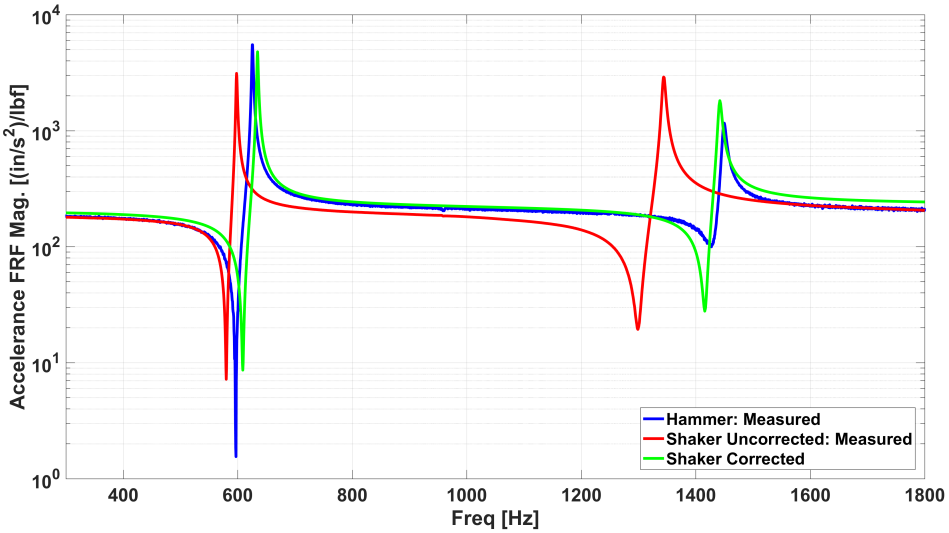

(a) Experimental drive-point FRF.

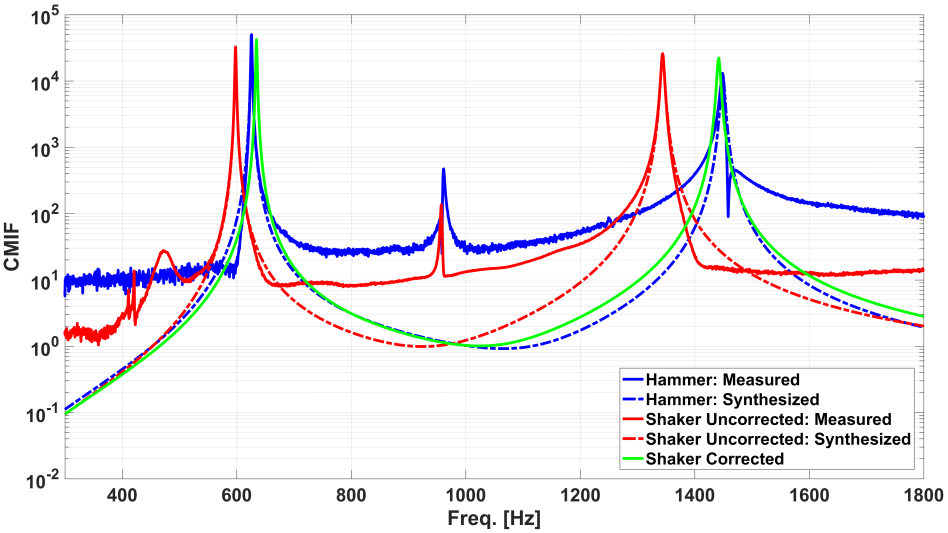

(b) Experimental CMIF with the measured (solid) and synthesized (dashed) values shown.

Figure 7: Frequency response for the two test configurations: the hammer test (blue) used as the truth baseline, and the shaker test with the attached force transducer assembly, both uncorrected (red) and corrected using the proposed approach (green).

an analytical model of this same section. Such constraints then enabled an estimation of the mode shapes for all degrees of freedom, including translations and rotations, at the transducer connection point. Knowledge of these connection point mode shapes allowed for the immediate removal of an analytical rigid body model of the transducer from the system, thus correcting the system dynamics. In the modal equations of motion, the removal of transducer mass and inertia at the connection point manifests itself as removal of an equivalent mass distributed across the measurement locations. Both numerical and experimental analysis on a T-Beam structure showed the feasibility of the proposed approach in correcting for both the modal frequency estimates, as well as the forced response.

Although the scope of the paper focused on the removal of the force transducer, the proposed approach may also be extended to remove the effects of other attached transducers, such as accelerometers, if necessary. If an analytical model for the entire test structure is known, e.g., when performing a modal test for model correlation, the proposed approach can enable full mode shape estimations at each transducer connection point allowing for the removal of all transducers simultaneously. Furthermore, it is imperative the analytical model of the local section forms a sufficient modal basis for estimating the transducer connection point mode shapes. The proposed approach does not rely on knowledge of the frequencies of the analytical model, so if an accurate model does not exist and is unable to be developed, one method to bypass this issue may be to estimate the mode shapes by curve-fitting polynomials through the measurement locations.

Acknowledgements

This work was supported by, and performed at Sandia National Laboratories. Sandia is a multimission laboratory managed and operated by National Technology and Engineering Solutions of Sandia, LLC., a wholly owned subsidiary of Honeywell International, Inc., for the U.S. Department of Energys National Nuclear Security Administration under contract DE-NA-0003525.

References

[1] D. J. Ewins, *Modal testing : theory, practice, and application*. Research Studies Press, 2000.

[2] J. Decker and H. Witfeld, "Correction of transducer-loading effects in experimental modal analysis," in *Proceedings of the 13th International Modal Analysis Conference*, 1995.

[3] J. M. M. Silva, N. M. M. Maia, and A. M. R. Ribeiro, "Some applications of coupling/uncoupling techniques in structural dynamics - part 1: Solving the mass cancellation problem," in *Proceedings of the 15th International Modal Analysis Conference*, (Orlando, FL), 1997.

[4] M. Ashory, "Correction of mass-loading effects of transducers and suspension effects in modal testing," in *Proceedings of the 16th International Modal Analysis Conference*, (Santa Barbara, CA), 1998.

[5] J. M. M. Silva, N. M. M. Maia, and A. M. R. Ribeiro, "Cancellation of mass-loading effects of transducers and evaluation of unmeasured frequency response functions," *Journal of Sound and Vibration*, vol. 236, no. 5, pp. 761–779, 2000.

[6] O. Cakar and K. Sanliturk, "Elimination of transducer mass loading effects from frequency response functions," *Mechanical Systems and Signal Processing*, vol. 19, no. 1, pp. 87–104, 2005.

[7] S. Bi, J. Ren, W. Wang, and G. Zong, "Elimination of transducer mass loading effects in shaker modal testing," *Mechanical Systems and Signal Processing*, vol. 38, no. 2, pp. 265–275, 2013.

[8] P. Zamani, A. T. Anbouhi, M. R. Ashory, M. M. Khatibi, and R. M. Nejad, "Cancelation of transducer effects from frequency response functions: Experimental case study on the steel plate," *Advances in Mechanical Engineering*, vol. 8, no. 4, pp. 1–12, 2016.

[9] K. G. McConnell and P. Cappa, "Transducer inertia and stinger stiffness effects on FRF measurements," *Mechanical Systems and Signal Processing*, vol. 14, no. 4, pp. 625–636, 2000.

[10] M. S. Allen and R. L. Mayes, "Comparison of FRF and modal methods for combining experimental and analytical substructures," in *Proceedings of the 25th International Modal Analysis Conference*, (Orlando, FL), 2007.

[11] M. S. Allen, R. L. Mayes, and E. J. Bergman, "Experimental modal substructuring to couple and uncouple substructures with flexible fixtures and multi-point connections," *Journal of Sound and Vibration*, vol. 329, no. 23, pp. 4891–4906, 2010.